PEDS Advance Access published October 20, 2015

Protein Engineering, Design & Selection, 2015, 1–9
doi: 10.1093/protein/gzv052
Original Article

OXFORD

Original Article

Reconstitution of the receptor-binding motif of the SARS coronavirus

Natalia T. Freund[1,4], Anna Roitburd-Berman[1], Jianhua Sui[2,3,5], Wayne A. Marasco[2,3], and Jonathan M. Gershoni[1,*]

[1]Department of Cell Research and Immunology, The George S. Wise Faculty of Life Sciences, Tel Aviv University, Tel Aviv 69978, Israel, [2]Department of Cancer Immunology and AIDS, Dana Farber Cancer Institute, [3]Department of Medicine, Harvard Medical School, Boston, MA 02115, USA, [4]Present address: Laboratory of Molecular Immunology, The Rockefeller University, New York, NY 10065, USA, and [5]Present address: National Institute of Biological Sciences, Beijing 102206, China

*To whom correspondence should be addressed. E-mail: gershoni@tauex.tau.ac.il
Edited by Dennis Burton

Received 27 July 2015; Revised 27 July 2015; Accepted 8 September 2015

Abstract

The severe acute respiratory syndrome (SARS) coronavirus (CoV) identified in 2003 has infected ~8000 people worldwide, killing nearly 10% of them. The infection of target cells by the SARS CoV is mediated through the interaction of the viral Spike (S) protein (1255 amino acids) and its cellular receptor, angiotensin-converting enzyme 2 (ACE2). The SARS CoV receptor-binding domain (amino acids N318–T509 of S protein) harbors an extended excursion along its periphery that contacts ACE2 and is designated the receptor-binding motif (RBM, amino acids S432–T486). In addition, the RBM is a major antigenic determinant, able to elicit production of neutralizing antibodies. Hence, the role of the RBM is a bi-functional bioactive surface that can be demonstrated by antibodies such as the neutralizing human anti-SARS monoclonal antibody (mAb) 80R which targets the RBM and competes with the ACE2 receptor for binding. Here, we employ phage-display peptide-libraries to reconstitute a functional RBM. This is achieved by generating a vast collection of candidate RBM peptides that present a diversity of conformations. Screening such 'Conformer Libraries' with corresponding ligands has produced short RBM constructs (ca. 40 amino acids) that can bind both the ACE2 receptor and the neutralizing mAb 80R.

Key words: bioactive peptide, conformational library, phage-display, virus spike

Introduction

The outbreak of the severe acute respiratory syndrome (SARS) epidemic in year 2002 (Rota *et al.*, 2003; Peiris *et al.*, 2004) motivated an international, WHO-coordinated collaborative effort to discover the etiologic agent of this emerging disease. By March 2003, this effort culminated with the discovery and cloning of the SARS coronavirus (SARS CoV) (Marra *et al.*, 2003; Rota *et al.*, 2003) and within the same year its receptor, angiotensin-converting enzyme 2 (ACE2) was identified (Li *et al.*, 2003). The SARS CoV Spike (S) binds to ACE2, which mediates viral infection (Li *et al.*, 2003). The S protein is a type 1, 1255-amino acid long transmembrane glycoprotein comprised of an N-terminal leader sequence (amino acids 1–12), a large extracellular domain (amino acids 13–1195) followed by a transmembrane segment (amino acids 1196–1215) and a relatively short cytoplasmic tail (amino acids 1216–1255) (Li *et al.*, 2005; Du *et al.*, 2009). The extracellular aspect of S protein can further be divided into two functional sub-domains; S1 responsible for receptor recognition (amino acids 13–666) and S2 (amino acids 667–1195), which in response to S1 binding to ACE2, undergoes conformational rearrangements that enable viral fusion with the target-cell membrane (Du *et al.*, 2009).

© The Author 2015. Published by Oxford University Press. All rights reserved. For Permissions, please e-mail: journals.permissions@oup.com

The receptor-binding domain (RBD) of CoVs in general can be located within the first few hundred amino acid residues of S1 (e.g. as in the mouse hepatitis virus (Dveksler *et al.*, 1991; Dveksler *et al.*, 1993; Kubo *et al.*, 1994)) or further downstream (e.g. as in human CoV 229E (Yeager *et al.*, 1992; Bonavia *et al.*, 2003; Breslin *et al.*, 2003)). The RBD of SARS CoV was identified as a minimal 193-amino acid long sequence starting around residue N318 (Xiao *et al.*, 2003; Babcock *et al.*, 2004; Wong *et al.*, 2004). However, efforts to produce smaller independently folding, functional receptor-binding peptides of S1 were unsuccessful (Babcock *et al.*, 2004; Wong *et al.*, 2004). The co-crystallization of the RBD bound to its receptor ACE2, revealed that the actual binding interface lies within an extended excursion juxtaposed along the edge of the core of the RBD and constitutes the receptor-binding motif (RBM, residues S432–T486) (Li *et al.*, 2005).

Several studies demonstrated that the SARS CoV RBM is targeted by a number of anti-SARS human antibodies (Sui *et al.*, 2004, 2005, 2008; Prabakaran *et al.*, 2006; Zhu *et al.*, 2007; Rockx *et al.*, 2008; Rockx *et al.*, 2010; Rani *et al.*, 2012), reviewed in Coughlin and Prabhakar (2012). One such antibody is the human monoclonal antibody (mAb) 80R, which neutralizes SARS CoV *in vitro* and *in vivo* (Sui *et al.*, 2004). The epitope of mAb 80R overlaps extensively with the binding surface recognized by ACE2, as is shown in the crystal structure of RBD/80R and by competition studies for binding to S1 domain (Sui *et al.*, 2004). Co-crystallization of mAb 80R with the RBD reveals that 9 of the 23 contact residues contained within the RBM coincide precisely with those that mediate ACE2 binding (Hwang *et al.*, 2006), illustrating the prominence of the RBM as a bi-functional bioactive surface.

Here, we describe the reconstitution of the SARS CoV RBM as an independently folding, functional binding domain of S1. A 41-amino acid peptide derived from the RBM is expressed in *Escherichia coli* and is shown to bind both ligands; the viral receptor ACE2 and the neutralizing mAb 80R.

Materials and methods

Vectors

The fth-1 vector was developed at Tel Aviv University as described in Enshell-Seijffers *et al.* (2001) and used to express inserts of choice at the N-terminus of the recombinant pVIII major coat protein of the fd filamentous bacteriophage.

Monoclonal antibodies and proteins

The human mAbs 80R (Sui *et al.*, 2004) and 11A (Sui *et al.*, 2008), which target the RBD of the SARS CoV, and the human ACE2 protein were produced at the Dana-Farber Cancer Institute, Boston, MA. Polyclonal rabbit anti-M13 sera and the recombinant pVIII-specific GIL-Ab (Kaplan and Gershoni, 2012) as well as the anti-m13 mAb Y2D (Siman-Tov *et al.*, 2013) were produced at Tel Aviv University.

Cloning of the RBM constructs

The initial RBM construct was produced by cloning residues S432–T486 of the RBD between the two SfiI restriction sites of the fth-1 recombinant *pVIII* gene. The 'loopless' RBM phage was prepared by cloning the two strands, $_{432}$STGNYNYKYRL$_{443}$ and $_{460}$FSPDGKPCTPCTPPALNCYWPLNDYGFYTT$_{486}$, contiguous to one another between the two SfiI restriction sites of the fth-1 recombinant *pVIII* gene. Using alternative codons, two unique restriction sites were introduced one in each strand; the restriction site for KpnI enzyme in the S432–L443 strand and the restriction site for ApaLI enzyme in the S460–T486 strand. In general, compatible oligonucleotides encoding the relevant construct were designed to create 5′ and 3′ overhangs compatible to the SfiI cloning sites of the fth-1 vector (Enshell-Seijffers *et al.*, 2001) and annealed to create double stranded inserts that were introduced into the SfiI-digested fth-1 vector; for details, see Freund *et al.* (2009).

Construction and analysis of 'Conformer Libraries'—phage-displayed RBM linker libraries

All linker libraries were cloned into the ApaLI and KpnI cloning sites of the 'loopless' RBM vector. Briefly, for the construction of the libraries, two 5′ biotinylated oligonucleotides were used. The first contained the 'library' sequence flanked by ApaLI and KpnI sites compatible with the ApaLI and KpnI cloning sites of the 'loopless' RBM vector. The second oligonucleotide complemented the 3′ end of the first and was extended to 'fill-in' the complementary strand using Klenow polymerase. The product was digested with ApaLI and KpnI, the short biotinylated segments were removed with streptavidin-conjugated beads, and the insert in the flow-through was collected and cloned into ApaLI and KpnI digested vector. This ligation mix was used to electroporate MC1061 cells; for details, see Freund *et al.* (2009). The randomness of each library was confirmed by sequencing 20–40 randomly picked colonies. The complexities of linker libraries with linkers comprised of NNK_1, NNK_2, NNK_3 and NNK_4 were 7.5×10^3, 5×10^6, 1.4×10^7 and 2×10^7, respectively.

Screening of 'Conformer Libraries'

Fifty micrograms of protein G (Sigma Chemical Co., St Louis, MO, USA) in Tris-buffered saline (50 mM Tris–HCl pH 7.5, 150 mM NaCl (TBS)) was used to coat the bottom of Costar 6-well tissue culture plates (Corning Incorporated, Corning, NY, USA) overnight at 4°C. The wells were blocked with 0.25% gelatin in TBS (TBSG), washed briefly with TBS, and then incubated with 20–70 μg/ml of mAb 80R at room temperature for at least 4 h. Unbound antibody was washed out with TBS, and the plate was incubated overnight at 4°C with 10^{11} phages from the phage-display library suspended in TBSG. After extensive washing, the mAb 80R-bound phages were eluted with glycine–HCl pH 2.2 and neutralized with Tris–HCl pH 9.1.

Two additional rounds of amplification and biopanning were carried out for each screen. In order to confirm mAb 80R binding to affinity-selected phages, single colonies were picked and grown as mini-cultures from which dot-blots on nitrocellulose membrane filters were prepared. The filters were blocked using 5% skim milk in TBS for 1 h at room temperature, probed with mAb 80R at 4°C (2 μg/ml) and subsequently detected using HRP-conjugated antibodies (1:5000, Jackson, West Grove, PA, USA). Signals were developed using the enhanced chemo-luminescence reaction (Rhenium, Israel). For details, see Freund *et al.* (2009).

Phage preparation

Phages displaying the peptides of interest were used to infect *E.coli* DH5αF' bacteria. The infected bacteria were grown overnight in 100 ml TYx2 medium with 20 μg/ml of tetracycline and then centrifuged to pellet bacteria. The phage-containing supernatants were transferred to PEG/NaCl solution and incubated at 4°C overnight to precipitate phages. Following centrifugation, the precipitated phages were re-suspended in TBS, filtered through a 0.45 μm filter and titered using a plaque assay.

Enzyme-linked immunosorbent assay tests

Nunc-Immuno Modules enzyme-linked immunosorbent assay (ELISA) wells (Nunc, Roskilde, Denmark) were coated overnight with 5–10 μg/ml of mAb 80R, or ACE2 in phosphate-buffered saline (PBS). Next, the plates were washed with PBS, blocked with 5% skim milk in PBS and incubated with a suspension of 10^{10} phages/well. Wells were washed with PBS and incubated with polyclonal rabbit anti-M13 antibody. Next, wells were washed and incubated with HRP-conjugated goat anti-rabbit antibody (1:5000, Jackson). Following an additional round of washing, wells were reacted with the TMB/E ELISA substrate (Merck Millipore, Billerica, MA, USA). Absorbance was measured at 650 nm using a micro-plate reader (BioTek, Winooski, VT, USA). All experiments were repeated at least three times and typically performed in duplicates.

Results

The atomic structure of the RBD has been solved at 2.9 and 2.3 Å resolution in complex with the ACE2 (Li *et al.,* 2005) and mAb 80R (Hwang *et al.,* 2006), respectively. The RBD structure from the mAb 80R co-crystal is depicted in Fig. 1A. As can be seen, residues I319–A430 create a compact core structure containing two glycosylation sites (N330, N357), two disulfide bonds (yellow bars) and a central anti-parallel beta sheet (β1–β4) (Fig. 1B and C). On one side of the beta sheet exists a series of three alpha helices (blue) and on the other side a looped structure, residues N393–F416 (red) (Fig. 1B). The RBM is an excursion spanning residues S432–T486 that lies on the edge of the core structure. The RBM contains two anti-parallel beta strands (β5 and β6, as indicated in Fig. 1A), a single disulfide bond and a 16-amino acid loop (green) that tacks the RBM to the core. Finally, an extended beta strand (β7, dark green) stems from residue Y491 to L504 back down through the core serving as a lynch-pin, hydrogen bonding with β3 and β4, and thus holding the entire structure together (Fig. 1C). It is no surprise that previous attempts to express functional RBDs missing residues N318–N330 and thereby disrupting the disulfide C323–C348 and devoid of β1, or truncations at residues G490 thus deleting the β7 lynch-pin, failed to produce independently folding stable and functional structures (see for example Babcock *et al.,* 2004; Wong *et al.,* 2004).

In examination of the RBD structure, one realizes that the vast majority of contacts with ACE2 and mAb 80R exist within the segment of the RBM residing between residues S432 and T486 (see Fig. 2A). Despite the extensive overlap between the contacts that interact with these two ligands, the methods by which they bind the RBM are very different. The ACE2 contacts 8 residues (spanning S432 to T486) of a total 10 via a single extended alpha helix (Q24–L45, see Fig. 2B) (Li *et al.,* 2005). In contrast to this, mAb 80R contacts 23 residues of the RBM via a series of 7 discontinuous segments derived from VH and VL domains (see Fig. 2C) (Hwang *et al.,* 2006). Both ligands bind the RBD with similar affinities (Sui *et al.,* 2004). In view of the more elaborate network of contacts employed by mAb 80R, it was decided to probe candidate RBM structures first with this antibody followed by subsequent evaluation of ACE2 binding.

Initially, the native structure, residues S432–T486, was cloned into the SfiI sites of the phage-display fth1 vector (Enshell-Seijffers *et al.,* 2001; Fig. 3). Despite the fact that this construct contained most of the ACE2 and mAb 80R contact residues no substantial binding for either ACE2 or mAb 80R could be demonstrated (see below).

In view of the fact that the 16-amino acid loop (residues R444–F459) located within the RBM does not contribute any contacts with the ligands and presumably functions only to tack the RBM to the core of the RBD, we postulated that it might cause some interference in the correct folding of the isolated binding surface. Hence, we removed the loop thus generating a 7 Å gap between residues L443 and F460 (Fig. 3). Simple closure of the gap by juxtaposing L443 directly to F460 did not produce a recognizable structure (see below). Furthermore, introduction of one, two, three or four glycine residues to bridge between L443 and F460, closing the gap with multiple glycine-linkers, was also ineffective in generating a functional RBM.

Consequently, we embarked on an empirical strategy proposing to identify functional linkers through affinity selection. Thus, we used mAb 80R as a probe to screen the 'loopless' RBM containing combinatorial linkers to bridge the L443/F460 gap. For this, all possible linkers of one to four residues were constructed and tested for mAb 80R binding. The rationale was that linkers consisting of one to four amino acids in length and comprised of all possible amino acid compositions would generate a comprehensive library of RBM conformers. Screening this library with mAb 80R would allow us to affinity select those constructs harboring a 'correct' linker length and composition that enables reconstitution of a functional binding surface. The cloning strategy used to construct the linker libraries and a summary of the library complexities are given in Fig. 3 and in 'Materials and methods' section, respectively. No mAb 80R binders were selected from screening libraries of 1-mer and 2-mer random linkers. Therefore, we conclude that although the entire theoretical complexity of linkers of 1 or 2 amino acids most probably was tested, none were able to effectively position the RBM-derived segments to assume a functional conformation. Numerous positive clones could, however, be affinity selected from both the 3-mer and 4-mer linker libraries. The amino acid sequences of the functional linkers were determined and compared as is illustrated in Fig. 4A. Of a total of 800 colonies of phage variants screened from the 3-mer and 4-mer linker libraries, 45 positive clones were identified representing 16 unique linkers. Most of the mAb 80R-selected linkers contained a glycine residue in the first position and a negatively charged E or D at position 2. For the 3-mer linkers, there was a propensity for residues E, N, P or M for the third position. The third position for the 4-mer linkers was typically P and greater variation for position 4 existed as is illustrated in Fig. 4A.

Figure 4B shows the comparative binding of mAb 80R to the various constructs. In order to enable meaningful comparison, it was first necessary to confirm that the constructs expressed equally on the phage surface. For this, we probed the different phages containing the various constructs with the GIL-Ab reagent (Kaplan and Gershoni, 2012) that specifically quantifies the level of recombinant pVIII in the bacteriophage, thus showing the expression of the constructs *per se* when compared with their ability to bind mAb 80R (Fig. 4B). We conclude that all constructs are expressed well on the phage surface and lack of binding is not due to lack of expression, as can be seen by comparing the initial RBM and 'loopless' RBM constructs to the GEM construct which are expressed in similar levels, however bind to mAb 80R very differently.

During the course of these analyses, we discovered a spontaneous point mutation at residue 465 from K to I (K465I) in some of the selected constructs. The mutated residue is not a contact residue for ACE2 or mAb 80R; however, this mutation seems to improve the binding of mAb 80R for some of the linkers. We discovered that reverting the K465I mutation to wild-type, i.e. replacing the aliphatic methyl of isoleucine to the original positive charge of lysine at position 465 led to a drop in binding activity for the two linkers tested, GEM465K and EEP465K (Fig. 5). No gain of binding was seen when the K465I mutation was introduced into the initial RBD

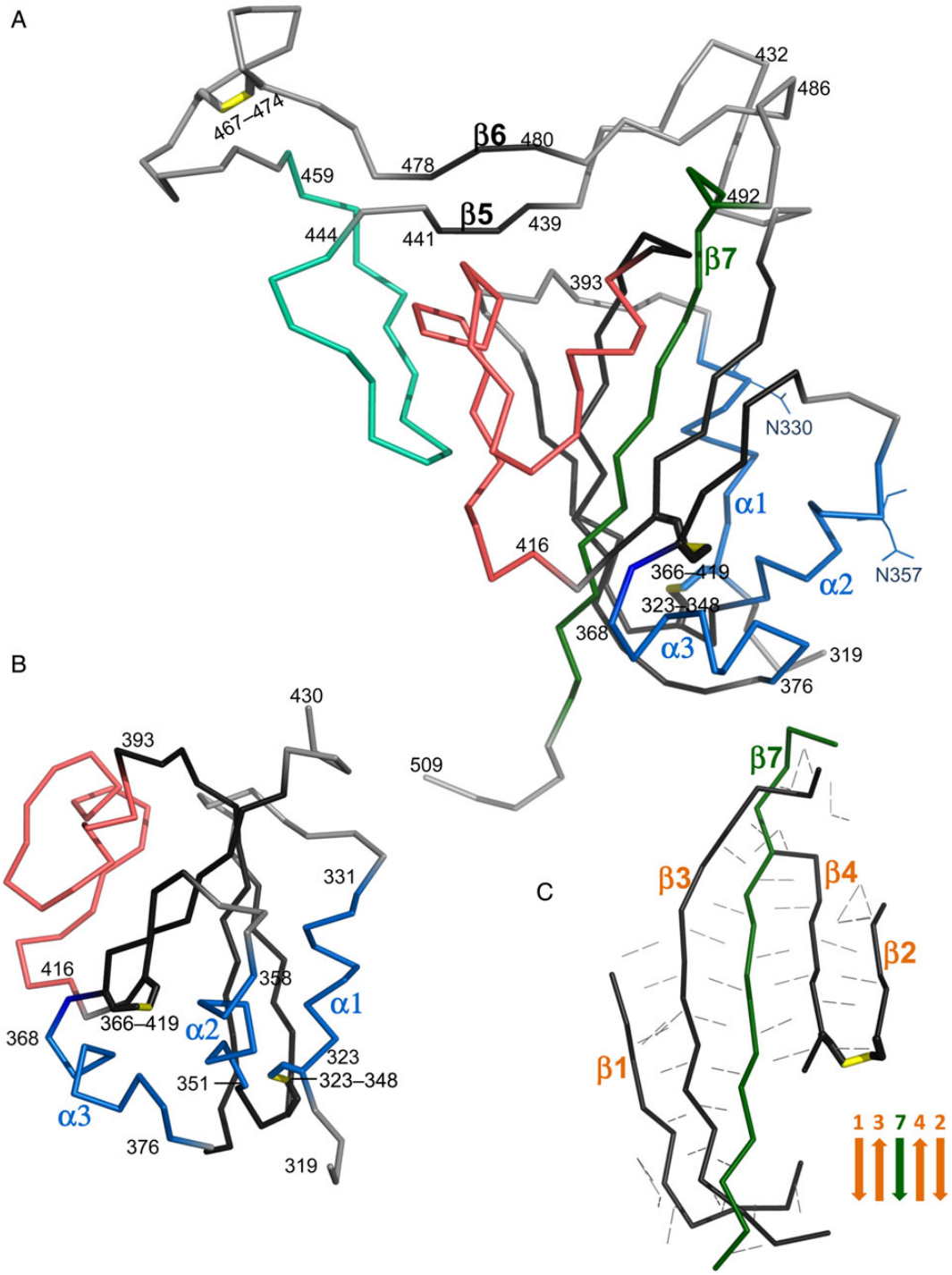

Fig. 1 The SARS CoV RBD. (**A**) A backbone representation of the SARS CoV RBD taken from the RBD/80R co-crystal (Hwang *et al.*, 2006) (PDBID: 2GHW, residues I319–T509, the mAb 80R is not shown). A series of three alpha helices (α1–α3, blue) and a looped structure (residues N393–F416, red) flank either side of the central anti-parallel beta sheet (β1–β4 + β7). For further details, see text. (**B**) A view of the RBD, residues I319–A430, has been rotated ~90° relative to 'a' to provide a clear view of α1–α3 (blue) bordering the compact central core structure. (**C**) Detail of the five beta strands (β1–β4 + β7) which are interconnected by a network of hydrogen bonds.

construct (data not shown). We also noticed that reverting the mutation for both positively selected constructs GEM and EEP resulted in a decrease of construct expression, as is indicated by GIL-Ab binding (Fig. 5). We conclude that K465I mutation is beneficial for mAb 80R binding and for the affinity selection of those phages containing it.

From mAb 80R, we tested the panel of functional RBM constructs against an additional 'antibody ligand', the neutralizing anti-SARS mAb 11A, which competes for ACE2 binding as well (Sui *et al.*, 2008). This antibody was isolated using the RBD from the late SARS CoV viral isolate, Guang Dong 03. Here too we found that

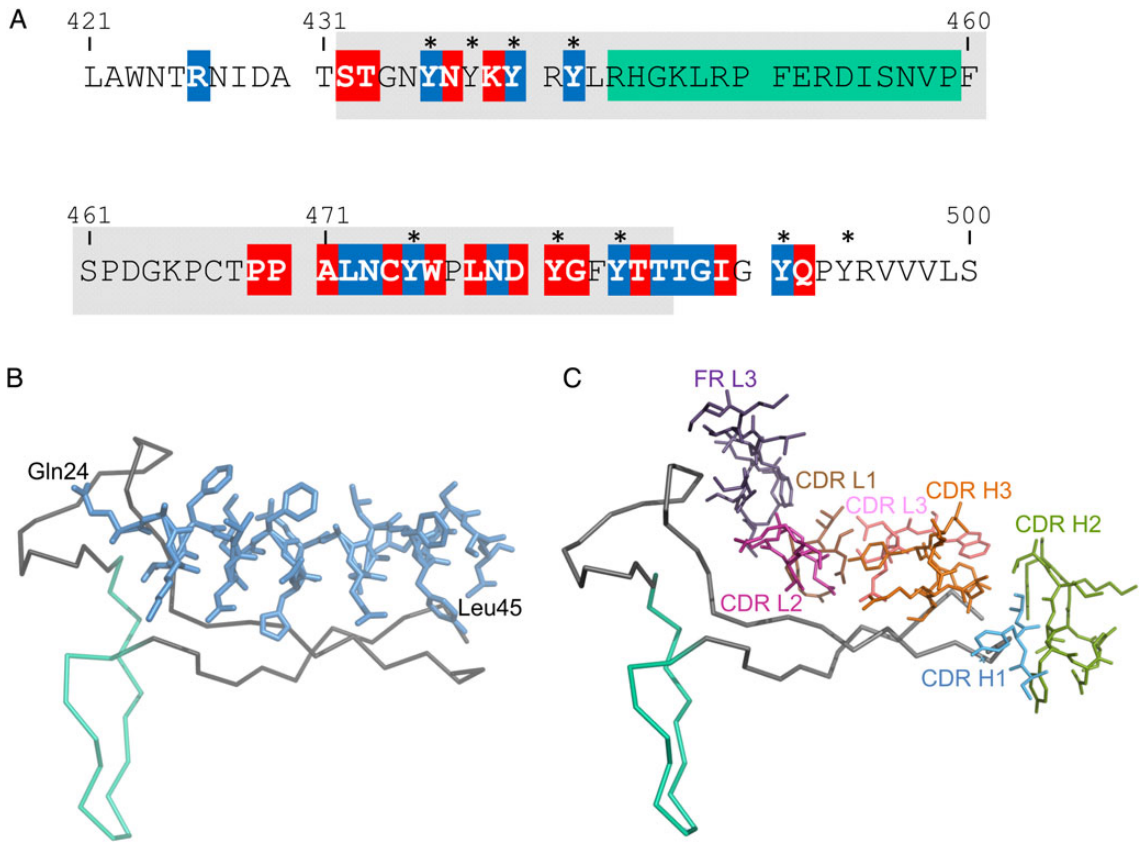

Fig. 2 ACE2 and mAb 80R RBD contact residues. (**A**) The RBD, L421–S500, contains a total of 29 residues that contact mAb 80R (red + blue), 16 of which are exclusive to mAb 80R (red, Hwang *et al.*, 2006) and additional 13 residues are shared by mAb 80R and ACE2 (blue, Li *et al.*, 2005). Residues of the 16-amino acid loop of the RBM (R444–P459) are highlighted in green. The amino acids of the RBM expressed in this study (S432–T486) are background highlighted. A total of nine tyrosine residues (marked with an asterisk) are shown, six of which are direct contact residues for both ACE2 and mAb 80R. (**B**) A single extended alpha helix of the ACE2 (PDBID: 2AJF; Q24–L45, light blue) (Li *et al.*, 2005) contacts eight residues of the RBM (residues S436–T486 in gray). (**C**) The mAb 80R contacts 28 residues of the RBM (PDBID: 2GHW; residues S432–T486 in gray) via a series of seven discontinuous segments (colored separately) (Hwang *et al.*, 2006). In **B** and **C**, the 16-amino acid loop is colored green.

the RBM harboring the GEM linker was specifically bound by mAb 11A (data not shown).

In view of this, we then proceeded to test whether mAb 80R-selected phages can bind to the SARS CoV natural receptor—ACE2, as well, thus further proving the bi-functional nature of the reconstituted structure (Fig. 6). Five of six linkers tested, with the exception of EEP linker, bound ACE2 well, with GEM being the best binder.

Discussion

The co-crystallization of the ACE2 with the SARS CoV RBD (Li *et al.*, 2005) revealed that the specific surface that mediates the binding is contained within an extended looped excursion separate and distinct from the core of the RBD. The RBM is a single sub-domain of the S1 protein that is tacked onto the core of the RBD via three hydrogen bonds contributed by the 16-amino acid loop extending perpendicular to the binding surface itself. Here, we have been able to reconstitute a functional RBM containing 9 of a total of 13 contact residues involved in ACE2 recognition (see Fig. 2A). This has been accomplished in two steps. First, it was hypothesized that the 16-amino acid loop was not only unnecessary for functional binding, but rather its presence hindered the functional folding of the RBM in the absence of the underlying core. Hence, this obstacle was removed. This, however, created a new problem, namely the need to bridge the gap between residues L443 and F460. The solution to this was to create libraries of combinatorial linkers and exploit the affinity selection using the mAb 80R as a probe. This proved to be extremely effective and numerous variations of reconstituted RBMs were produced. The fact that the novel structures were recognized by three independent conformation-sensitive probes (mAbs 80R and 11A and the natural receptor ACE2) gives credence to the conclusion that isolated RBM, detached from the core of RBD, can fold independently and assume the functional conformation required for receptor and antibody binding, provided the 'correct' linker is implemented to bridge the L443–F460 gap.

Since the discovery of the RBD, a number of attempts have been made to produce small peptide ligands that can bind ACE2 or act as inhibitors of viral entry via ACE2 (Hu *et al.*, 2005; Ho *et al.*, 2006; Struck *et al.*, 2012; Chang *et al.*, 2014). Indeed, a few of such peptides have been reported that seem to bind ACE2 at micro-molar concentrations (Ho *et al.*, 2006; Struck *et al.*, 2012). Two of these peptides are particularly interesting in view of the fact that they correspond to specific segments of the RBM. Thus for example, Struck *et al.* reported that the sequence 438–443 (YKYRYL) of the RBM binds ACE2 and can interfere with SARS CoV infection of Vero cells (Struck *et al.*, 2012). Similarly, Ho *et al.* published that the 12mer peptide 483-FYTTTGIGYQPY-494 is able to bind ACE2 as well (Ho *et al.*, 2006). Both these peptides contain three tyrosine residues derived

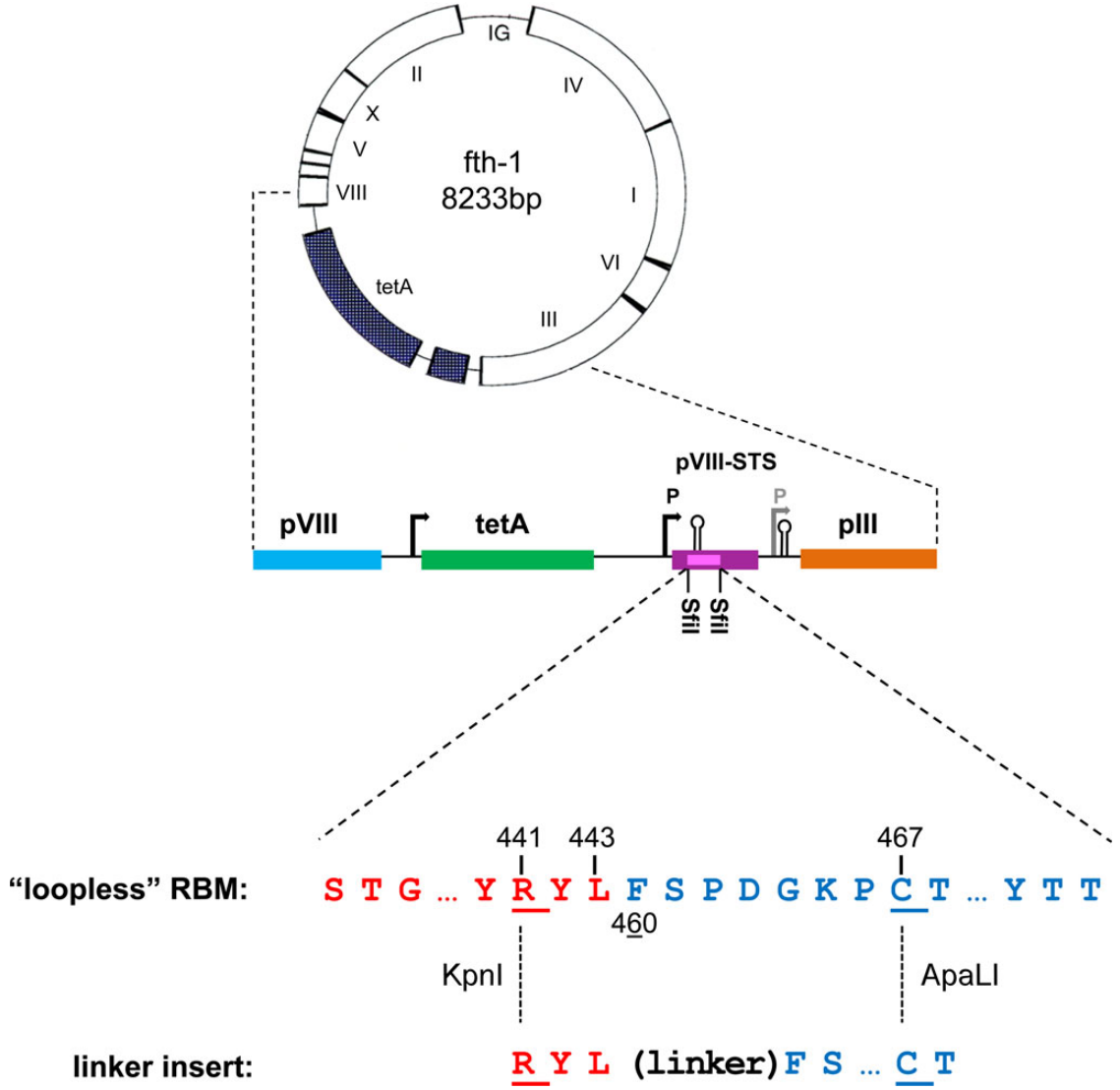

Fig. 3 Cloning strategy of the different RBM constructs. A schematic representation of the fth-1 vector; both the wild-type and recombinant (pVIII-STS) copy of the protein VIII (*pVIII*) genes are shown (blue and violet, respectively). The recombinant protein VIII gene contains a DNA stuffer that encodes for two stop codons and an RNA transcription terminator (hairpin structure), promoters are also indicated (Enshell-Seijffers *et al.*, 2001). The stuffer is removed when an insert is cloned between the two SfiI sites. The two segments of the RBM (residues S432–L443 and F460–T486) were cloned into the recombinant *pVIII* gene generating a 'loopless' RBM phage (the 16-amino acid loop is deleted, thus connecting the two segments of the RBM directly). Two unique restriction sites, KpnI and ApaLI, flanking the deleted 'loop' are shown. For more details, see 'Materials and methods' section.

from the RBM sequence (Y494 lies just beyond the RBM). Note that a total of nine tyrosines are interspersed along the RBM extended loop (marked with an asterisk in Fig. 2A and shown in Fig. 7) and six of them are used as contact residues for both ACE2 and mAb 80R (see Fig. 2A and Li *et al.*, 2005). The special contribution of tyrosine residues to functional binding sites has been reported and exploited for the production of novel antibodies. Sidhu and co-workers illustrate that high-affinity recombinant antibodies can be produced in which the CDR loops are comprised of various combinations of four amino acids (YADS, Fellouse *et al.*, 2004) or exclusively with only serine and tyrosine (Fellouse *et al.*, 2005). Hence, it may not be surprising that short peptides bearing three inter-spaced tyrosines can associate with ACE2, provided that they are unrestricted at their ends and free to assume unconstrained conformations, some of which may be able to adapt to the ACE2 helix. The fact remains, however, that all previous attempts to express the truncated RBDs (Babcock *et al.*, 2004; Wong *et al.*, 2004), as well as our initial attempts to reconstitute the RBM, failed to produce effective binders despite the presence of the same tyrosine-rich sequences of the RBM. Thus, one can conclude that the linear sequence of the RBM must fold into the correct conformation in order to assume a functional binding surface.

The production of comprehensive 'Conformer Libraries' has proved effective in the effort of reconstituting functional RBMs. These libraries express constant compositions and sequences of the RBM *per se* yet differ in the details of their three-dimensional conformations. This is accomplished by implementing a vast collection of random combinatorial linkers varying in length and composition. The affinity selection of conformers that satisfy the spatial orientation and display of the native contact residues has proved very efficient. The credence of this method is supported by the fact that three independent

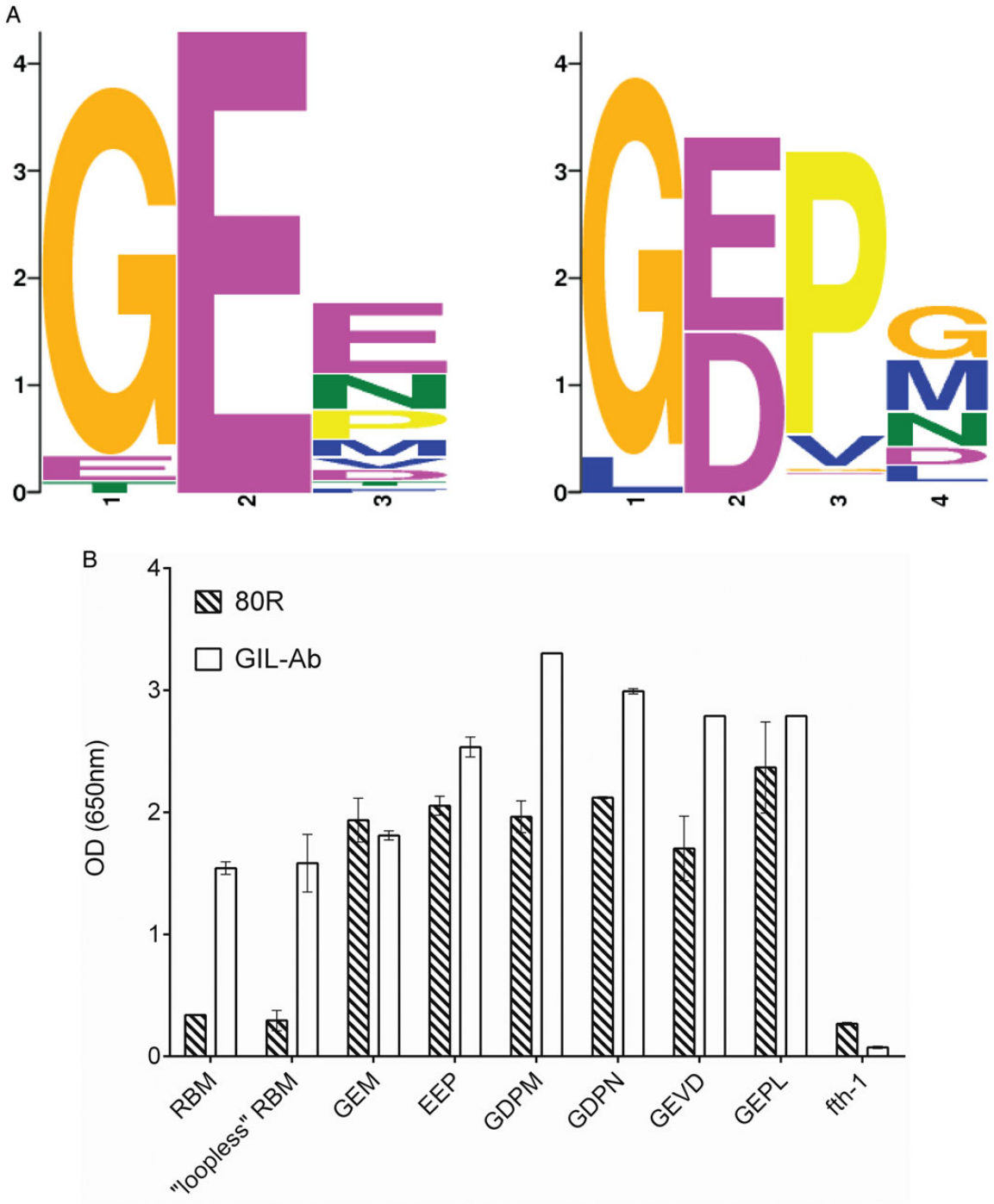

Fig. 4 Sequence analysis of RBM linker libraries and binding of affinity-selected phages to mAb 80R. (**A**) The sequences of linkers which were affinity selected using mAb 80R from NNK_3 and NNK_4 RBM 'Conformer Libraries' (left and right logos, respectively) were used as input for the MEME Suite motif analysis software (the MEME Suite: http://meme.sdsc.edu/meme, Bailey *et al.*, 2009). The MEME logos illustrate the amino acid distribution in the affinity-selected linkers. (**B**) ELISA demonstrating the binding of affinity-selected phages to mAb 80R. The overall expression of RBM peptides in each case is measured using the GIL-Ab reagent (Kaplan and Gershoni, 2012), wild-type phage fth-1 was used as a negative control. Error bars show SD.

conformation-specific probes bind constructs incorporating the same linkers. These three probes represent two very different modes of interaction with an extended surface of the RBM (Fig. 2B and C). As is illustrated, the natural ligand, i.e. the viral receptor, ACE2, employs a single continuous helix that contacts 10 residues, 8 of which are contained within the RBM (spanning S432–T486), and no contacts within the 16-amino acid structural loop (Fig. 2B, highlighted green) (Li *et al.*, 2005). The mAb 80R, on the other hand, uses a totally different mode of recognition (Fig. 2C). All three CDR loops of the heavy chain and two CDR loops of the light chain in addition to two discontinuous segments of the framework contribute 23 contact residues (9 common with those contacting ACE2). Once again no contacts are

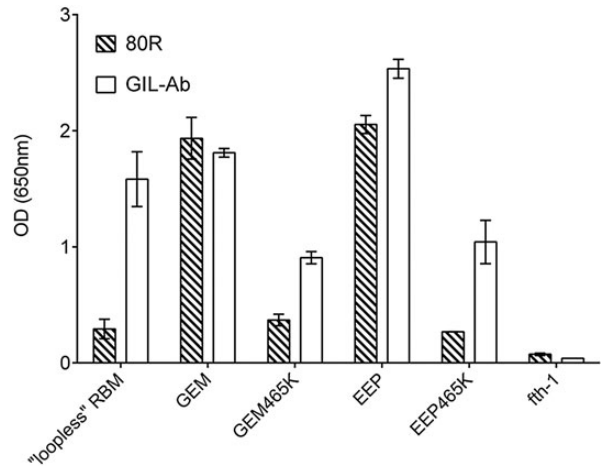

Fig. 5 The impact of the K465I mutation on expression and binding of affinity-selected phages GEM and EEP to mAb 80R. The binding of wild-type GEM465K and EEP465K phages to mAb 80R was compared with that of affinity-selected GEM and EEP in which lysine 465 spontaneously mutated to isoleucine. The overall expression of RBM peptides in each case is measured using the GIL-Ab reagent, wild-type phage fth-1 was used as a negative control. Error bars show SD.

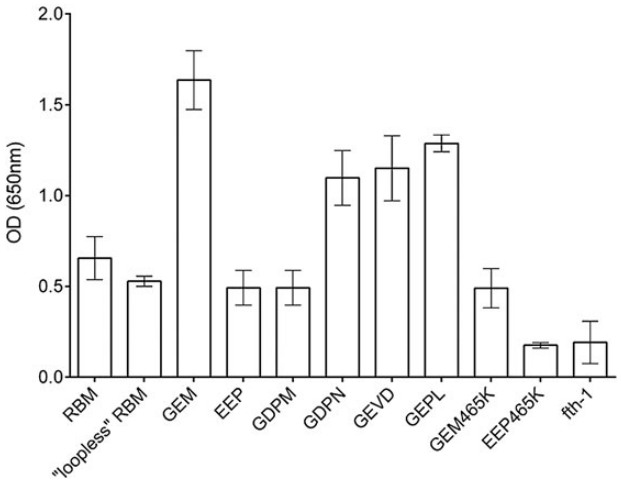

Fig. 6 Binding of mAb 80R affinity-selected phages to the ACE2 receptor. ELISA demonstrating the binding of immobilized human ACE2 protein to affinity-selected phages. Binding of phages to the ACE2 protein was detected using polyclonal rabbit antibodies specific to M13. Error bars show SD.

made with the 16-amino acid loop (Fig. 2C, highlighted green) (Hwang *et al.*, 2006). Hence, we conclude that the affinity-selected linkers in their ability to satisfy such diverse ligand interactions must enable the RBM to assume its natural conformation. Moreover, the fact that the linkers themselves represent a common motif goes to illustrate that a distinct structure and composition of linker is required so to place the contact residues in register and position to be complemented by the binding counter-parts.

Previously, we have developed the means to map neutralizing epitopes as a first step in the development of 'epitope-based vaccines' (Bublil *et al.*, 2006; Tarnovitski *et al.*, 2006; Bublil *et al.*, 2007; Gershoni *et al.*, 2007; Mayrose *et al.*, 2007a,b; Rubinstein *et al.*, 2008). The next task in such an effort requires the ability to produce the neutralizing epitopes as independently folded and functional

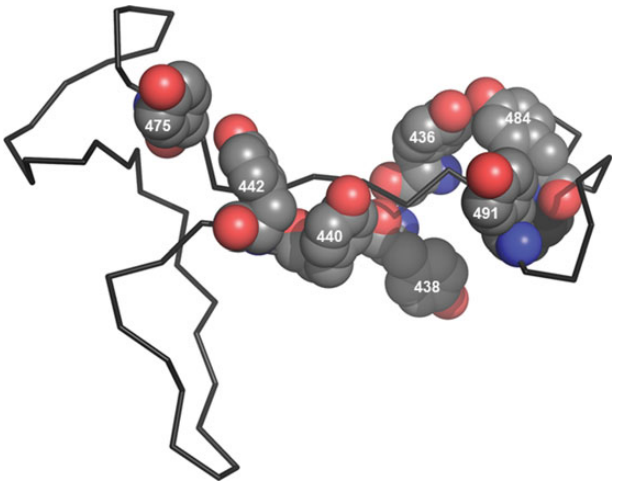

Fig. 7 The distribution of tyrosine residues throughout the RBM. A total of seven tyrosine residues (space-fill) are interspersed along the RBM, six of which are direct contact residues for both ACE2 and mAb 80R (see also Fig. 2).

bioactive peptides. Here, we have illustrated that 'Conformer Libraries' can assist in the affinity selection of functional binding surfaces. Future studies will go to test the next step of epitope-based vaccine development, i.e. are the reconstituted binding surfaces immunogenic and can they elicit protective immunity?

Acknowledgements

Conflict of interest: J.M.G. is the incumbent of the David Furman Chair of Immunobiology in Cancer. A.R.-B. received the Dan David Doctoral Fellowship. N.T.F. received the Clore Israel Foundation Scholarship. N.T.F. and A.R.-B. were recipients of the Jakov, Miriana and Jorge Saia Doctoral Fellowship.

Funding

This work has been supported by a grant from the US-Israel Binational Science Foundation [2005290 to J.M.G. and W.A.M].

References

Babcock,G.J., Esshaki,D.J., Thomas,W.D., Jr. and Ambrosino,D.M. (2004) *J. Virol.*, **78**, 4552–4560.

Bailey,T.L., Boden,M., Buske,F.A., Frith,M., Grant,C.E., Clementi,L., Ren,J., Li,W.W. and Noble,W.S. (2009) *Nucleic Acids Res.*, **37** (Web Server issue), W202–W208.

Bonavia,A., Zelus,B.D., Wentworth,D.E., Talbot,P.J. and Holmes,K.V. (2003) *J. Virol.*, **77**, 2530–2538.

Breslin,J.J., Mork,I., Smith,M.K., *et al.* (2003) *J. Virol.*, **77**, 4435–4438.

Bublil,E.M., Yeger-Azuz,S. and Gershoni,J.M. (2006) *FASEB J.*, **20**, 1762–1774.

Bublil,E.M., Freund,N.T., Mayrose,I., Penn,O., Roitburd-Berman,A., Rubinstein,N.D., Pupko,T. and Gershoni,J.M. (2007) *Proteins*, **68**, 294–304.

Chang,H.H., Chen,P.K., Lin,G.L., Wang,C.J., Liao,C.H., Hsiao,Y.C., Dong, J.H. and Sun,D.S. (2014) *J. Virol. Methods*, **201**, 1–6.

Coughlin,M.M. and Prabhakar,B.S. (2012) *Rev. Med. Virol.*, **22**, 2–17.

Du,L., He,Y., Zhou,Y., Liu,S., Zheng,B.J. and Jiang,S. (2009) *Nat. Rev. Microbiol.*, **7**, 226–236.

Dveksler,G.S., Pensiero,M.N., Cardellichio,C.B., Williams,R.K., Jiang,G.S., Holmes,K.V. and Dieffenbach,C.W. (1991) *J. Virol.*, **65**, 6881–6891.

Dveksler,G.S., Dieffenbach,C.W., Cardellichio,C.B., McCuaig,K., Pensiero,M.N., Jiang,G.S., Beauchemin,N. and Holmes,K.V. (1993) *J. Virol.*, **67**, 1–8.

Enshell-Seijffers,D., Smelyanski,L. and Gershoni,J.M. (2001) *Nucleic Acids Res.*, **29**, E50–E50.

Fellouse,F.A., Wiesmann,C. and Sidhu,S.S. (2004) *Proc. Natl Acad. Sci. U.S.A.*, **101**, 12467–12472.

Fellouse,F.A., Li,B., Compaan,D.M., Peden,A.A., Hymowitz,S.G. and Sidhu, S.S. (2005) *J. Mol. Biol.*, **348**, 1153–1162.

Freund,N.T., Enshell-Seijffers,D. and Gershoni,J.M. (2009) *Curr. Protoc. Immunol.*, Chapter 9, 9.8.1–9.8.30.

Gershoni,J.M., Roitburd-Berman,A., Siman-Tov,D.D., Tarnovitski Freund,N. and Weiss,Y. (2007) *BioDrugs*, **21**, 145–156.

Ho,T.Y., Wu,S.L., Chen,J.C., Wei,Y.C., Cheng,S.E., Chang,Y.H., Liu,H.J. and Hsiang,C.Y. (2006) *Antiviral Res.*, **69**, 70–76.

Hu,H., Li,L., Kao,R.Y., *et al.* (2005) *J. Comb. Chem.*, **7**, 648–656.

Hwang,W.C., Lin,Y., Santelli,E., Sui,J., Jaroszewski,L., Stec,B., Farzan,M., Marasco,W.A. and Liddington,R.C. (2006) *J. Biol. Chem.*, **281**, 34610–6.

Kaplan,G. and Gershoni,J.M. (2012) *Anal. Biochem.*, **420**, 68–72.

Kubo,H., Yamada,Y.K. and Taguchi,F. (1994) *J. Virol.*, **68**, 5403–5410.

Li,W., Moore,M.J., Vasilieva,N., *et al.* (2003) *Nature*, **426**, 450–454.

Li,F., Li,W., Farzan,M. and Harrison,S.C. (2005) *Science*, **309**, 1864–1868.

Marra,M.A., Jones,S.J., Astell,C.R., *et al.* (2003) *Science*, **300**, 1399–1404.

Mayrose,I., Shlomi,T., Rubinstein,N.D., Gershoni,J.M., Ruppin,E., Sharan,R. and Pupko,T. (2007a) *Nucleic Acids Res*, **35**, 69–78.

Mayrose,I., Penn,O., Erez,E., *et al.* (2007b) *Bioinformatics*, **23**, 3244–3246.

Peiris,J.S., Guan,Y. and Yuen,K.Y. (2004) *Nat. Med.*, **10** (12 Suppl), S88–S97.

Prabakaran,P., Gan,J., Feng,Y., Zhu,Z., Choudhry,V., Xiao,X., Ji,X. and Dimitrov,D.S. (2006) *J. Biol. Chem.*, **281**, 15829–15836.

Rani,M., Bolles,M., Donaldson,E.F., Van Blarcom,T., Baric,R., Iverson,B. and Georgiou,G. (2012) *J. Virol.*, **86**, 9113–9121.

Rockx,B., Corti,D., Donaldson,E., Sheahan,T., Stadler,K., Lanzavecchia,A. and Baric,R. (2008) *J. Virol.*, **82**, 3220–3235.

Rockx,B., Donaldson,E., Frieman,M., Sheahan,T., Corti,D., Lanzavecchia,A. and Baric,R.S. (2010) *J. Infect. Dis.*, **201**, 946–955.

Rota,P.A., Oberste,M.S., Monroe,S.S., *et al.* (2003) *Science*, **300**, 1394–1399.

Rubinstein,N.D., Mayrose,I., Halperin,D., Yekutieli,D., Gershoni,J.M. and Pupko,T. (2008) *Mol. Immunol.*, **45**, 3477–3489.

Siman-Tov,D.D., Zemel,R., Tur Kaspa,R. and Gershoni,J.M. (2013) *Anal. Biochem.*, **432**, 63–70.

Struck,A.W., Axmann,M., Pfefferle,S., Drosten,C. and Meyer,B. (2012) *Antiviral Res.*, **94**, 288–296.

Sui,J., Li,W., Murakami,A., *et al.* (2004) *Proc. Natl Acad. Sci. U.S.A.*, **101**, 2536–2541.

Sui,J., Li,W., Roberts,A., *et al.* (2005) *J. Virol.*, **79**, 5900–5906.

Sui,J., Aird,D.R., Tamin,A., *et al.* (2008) *PLoS Pathog*, **4**, e1000197.

Tarnovitski,N., Matthews,L.J., Sui,J., Gershoni,J.M. and Marasco,W.A. (2006) *J. Mol. Biol.*, **359**, 190–201.

Wong,S.K., Li,W., Moore,M.J., Choe,H. and Farzan,M. (2004) *J. Biol. Chem.*, **279**, 3197–3201.

Xiao,X., Chakraborti,S., Dimitrov,A.S., Gramatikoff,K. and Dimitrov,D.S. (2003) *Biochem. Biophys. Res. Commun.*, **312**, 1159–1164.

Yeager,C.L., Ashmun,R.A., Williams,R.K., Cardellichio,C.B., Shapiro,L.H., Look,A.T. and Holmes,K.V. (1992) *Nature*, **357**, 420–422.

Zhu,Z., Chakraborti,S., He,Y., *et al.* (2007) *Proc. Natl Acad. Sci. U.S.A.*, **104**, 12123–12128.